Design and Construction

Study on the Tensioning Scheme for Construction Monitoring of Asymmetric Single-Tower Cable-Stayed Bridges

Quan Zhang [1], Xianjing Li [2,*], Jishu Wu [1] and Chao Liu [1]

[1] Department of Bridge Engineering, Tongji University, Shanghai 200092, China;
[2] Lin Tung-Yen & Li Guo-Hao Consultants Shanghai Co., Ltd., Shanghai 202150, China;
* Correspondence: 820100664@qq.com

Abstract: Cable-stayed bridges, due to their unique mechanical structure, have the ability to span larger distances, therefore, they are increasingly emphasized in modern bridge construction. With the continuous improvement of engineering requirements, cable-stayed bridges have gradually become a primary bridge type for long-span structures. Due to the complexity of cable-stayed bridge structures, to ensure that the actual construction state of the bridge is close to optimal, the bridge must be strictly monitored and controlled during construction. In this paper, Jinwu Bridge in Jinhua, Zhejiang Province, is taken as the research background. This bridge is an asymmetric single-tower cable-stayed bridge. The spans and materials of the main girders on both sides of the bridge pylons are different. During the tensioning of stay cables, the space effect of the main girder is prone to generating an unbalanced moment. Herein, a study on the tensioning scheme of stay cables is carried out. The results show that, compared with those of the one-time tensioning scheme for stay cables, the stress state and cable force of the bridge are better when the two-time tensioning scheme is used, meeting the construction monitoring requirements.

Keywords: Asymmetric cable-stayed bridge; finite element calculation; construction monitoring

Citation: Zhang, Q.; Li, X.; Wu, J.; Liu, C. Study on the Tensioning Scheme for Construction Monitoring of Asymmetric Single-Tower Cable-Stayed Bridges. *Prestress Technology* **2023**, *3*, 70-81. https://doi.org/10.59238/j.pt.2023.03.006

Received: 26/11/2023
Accepted: 15/12/2023
Published: 25/12/2023

1 Introduction

In recent years, with the continuous development of transportation in China, an increasing number of cable-stayed bridges with strong spanning ability and graceful landscape effects have been developed [1]. The construction of cable-stayed bridges is complicated, and the process itself and its quality determine the state of the completed bridge. Scholars have conducted in-depth studies on the adjustment of construction cable forces and proposed a series of methods for optimizing the cable forces of cable-stayed bridges. These methods can be roughly divided into reverse disassembly method, reverse disassembly to positive installation method, positive installation iteration method, and zero-stress state control methods [2-5]. In addition, determining and optimizing the tensioning scheme to maintain good stress-bearing conditions in cable-stayed bridges and to rationally design bridges are keys in the construction of cable-stayed bridges. To analyze a symmetric cable-stayed bridge, Wei et al. [6] optimized the cable tensioning scheme by improving the construction method so that the structural state of the bridge can meet the code requirements after the bridge is completed. Duan et al. [7] optimized the tensioning scheme of a cable-stayed bridge by the reliability-based structural optimization method to ensure the safe stress-bearing state and construction efficiency of the structure. However, most recent studies involve symmetric cable-stayed bridges. Due to their complex structures, asymmetric cable-stayed bridges are prone to generate unbalanced moments. Moreover, the tension scheme has a more significant effect on the overall load bearing of the bridge; thus, further analysis and study are needed.

In this paper, by taking the Jinwu Bridge in Jinhua City, Zhejiang Province, as the research background, the tension scheme of an asymmetric cable-stayed bridge is studied. The Jinwu Bridge uses ultrawide bilateral girders with many stay cables, and the space effect of the structure during the tensioning process is significant. In this study, from the perspective of construction monitoring, a finite element model is created for calculation. Then, the control indicators of the structure are compared and analyzed by changing the number of tensioning cycles and the tensioning cable force of the stay cables, thereby determining the optimal tensioning scheme.

2 Project Overview

The total length of the Jinwu Bridge is 228 m, the span arrangement is 85 m+143 m, and the bridge width is 40 m. The main tower adopts an arched tower column, which represents the separation zone of motorized and non-motorized vehicle and has a special-shaped box cross-section. The main girders on both sides of the bridge tower are made of concrete bilateral girders and steel box girders. The junction surface between the steel girder and concrete girder is at the side of the main span at a distance of 15.5 m from the centerline of the main tower. The concrete beams are paved with 6.6-cm-thick C50 concrete + 5-cm-thick asphalt concrete; the steel beams are paved with 5-cm-thick Ultra-High-Performance Concrete (UHPC) + 5-cm-thick asphalt concrete.

A tower pier-beam consolidation system is adopted in the design. The main tower has a concrete structure below the bridge deck with a height of 13.511 m; the steel structure above the bridge deck is 82.121 m in height. There are a total of 60 stay cables across the bridge. The stay cables adopt a fan-shaped spatial dual-cable surface system, and the stay cables are high-strength parallel steel wires. The standard vertical anchor spacing of the stay cables is 5 m in the concrete beam section and 9 m in the steel beam section; the standard vertical anchor spacing on the tower is 2.5 m. The stay cables are anchored on the beam at the root of the cantilever, the anchor blocks are set in the anchorage area of the concrete beam section, and the steel anchor boxes are set in the anchorage area of the steel beam and steel tower.

The Jinwu Bridge adopts hinged joint system-based coordinated rotation construction technology for large-tonnage steel towers and temporary supports including the horizontal segmental assembly of the main tower on the bridge deck, the compression bar trusses assembled on the supports, and the vertical rotation construction of the arched main tower. The arched steel structure main tower weighs 2,148 tons, the total weight of the main tower is 2,530 tons in vertical rotation, and the tower height is 82.4 meters. To date, the steel tower in China has the largest vertical rotation construction weight among similar bridges.

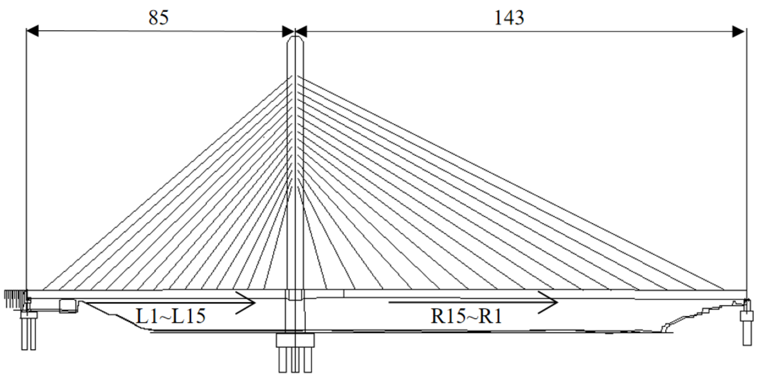

(a) Elevation plan of the main bridge

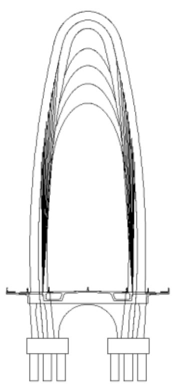

(b) Elevation diagram of the main tower

Figure 1 Bridge elevation (Unit: m)

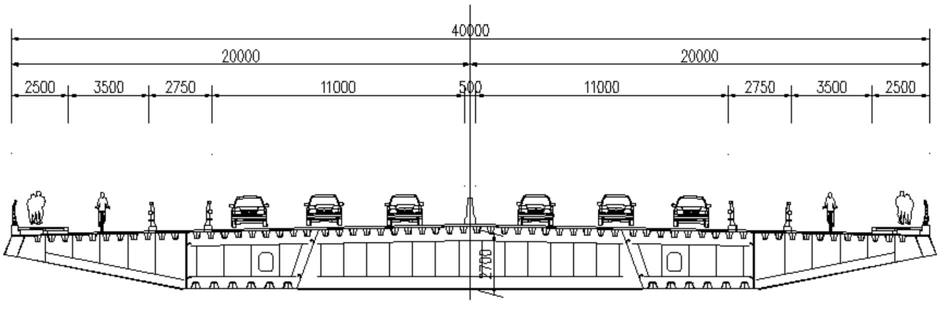

(a) Steel box girder section

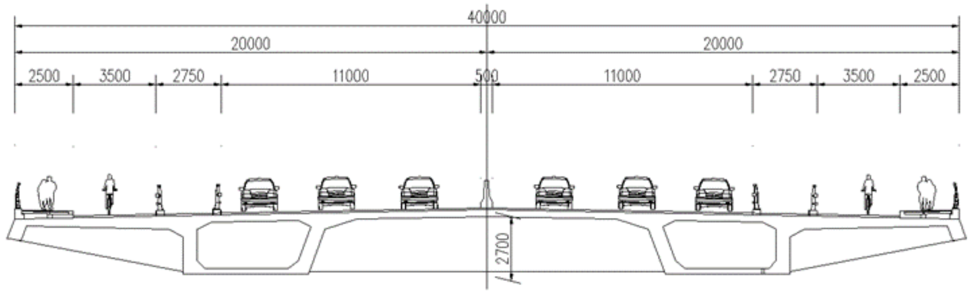

(b) Concrete box girder section

Figure 2 Cross-sectional diagram of the main bridge (Unit: m)

On September 6, 2022, the reconstructed Jinwu Bridge was officially opened to traffic, and the completed bridge is shown in Figure 3.

Figure 3 Image of the Jinwu Bridge after it was completed

3 Study on the tensioning scheme of stay cables

3.1 Finite element model construction

The Midas/Civil software was employed for modeling and analysis. The main bridge computational model, as shown in Figure 4, utilized both beam elements and tension-only cable elements to analyze the main bridge. The main bridge model of the Jinwu Bridge comprises a total of 1247 nodes and 1375 elements. Among these, there are a total of 1315 beam elements and 60 tension-only cable elements. Both the concrete and steel main girders were modeled using a double-beam model. The overall coordinate system for the bridge was defined as follows: the x-axis is longitudinal to the bridge, the y-axis is transverse to the bridge, and the z-axis is vertical. The bridge tower and main girders were simulated using beam elements, while the stay cables were simulated using tension-only cable elements. The simulation of boundary conditions includes:

(1) The bottom of the bridge tower is fixed, connecting directly with the beams at the junction.
(2) At the bridge piers, nodes are established at the actual support positions, and the corresponding degrees of freedom are constrained according to the drawings. Elastic connection rigidity is set between the support nodes and beam nodes.
(3) Elastic connection rigidity is applied for the connection between the stay cables and beams, as well as between the stay cables and bridge towers.

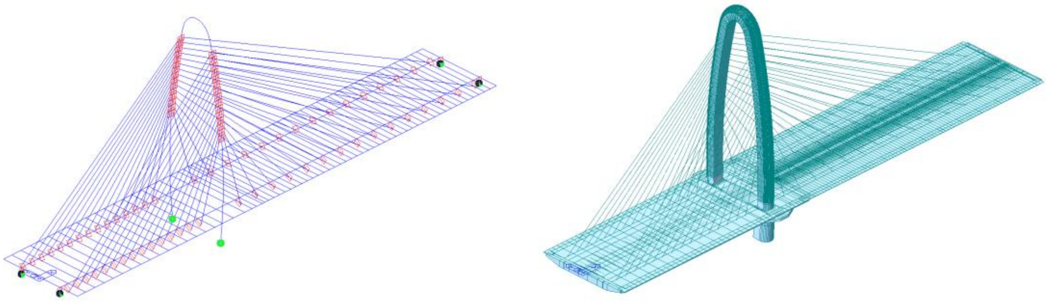

(a) Nodal element diagram (b) Rendered image

Figure 4 Midas model diagram

3.2 Comparison of tensioning schemes

During the construction of cable-stayed bridges, multiple system conversions are needed. The tensioning of stay cables is the most critical process; this tensioning not only meets the load-bearing safety requirements of the structure during the tensioning process but also satisfies the ideal bridge forming state.

After considering the various schemes, two reasonable tensioning schemes were ultimately selected for comparison. In the first tensioning scheme, after tensioning the stay cables in the sequence from L15, R15 to L1, R1, proceed with the installation of UHPC pavement and guardrails. Finally, dismantle the supports to achieve the completed bridge state. The second tensioning scheme is generally divided into two steps. (1) Tensioning is first performed sequentially from L15 to L1 and from R15 to R1 to 50% of the target cable force. (2) After the completion of the asphalt pavement and guardrail installation, the second tensioning process is carried out; tension is applied from L1 to L15 and from R1 to R15 to the target cable force. After completing the tensioning, remove the supports to achieve the finalized bridge state. The finite element calculation process for the construction site is shown in Figure 5.

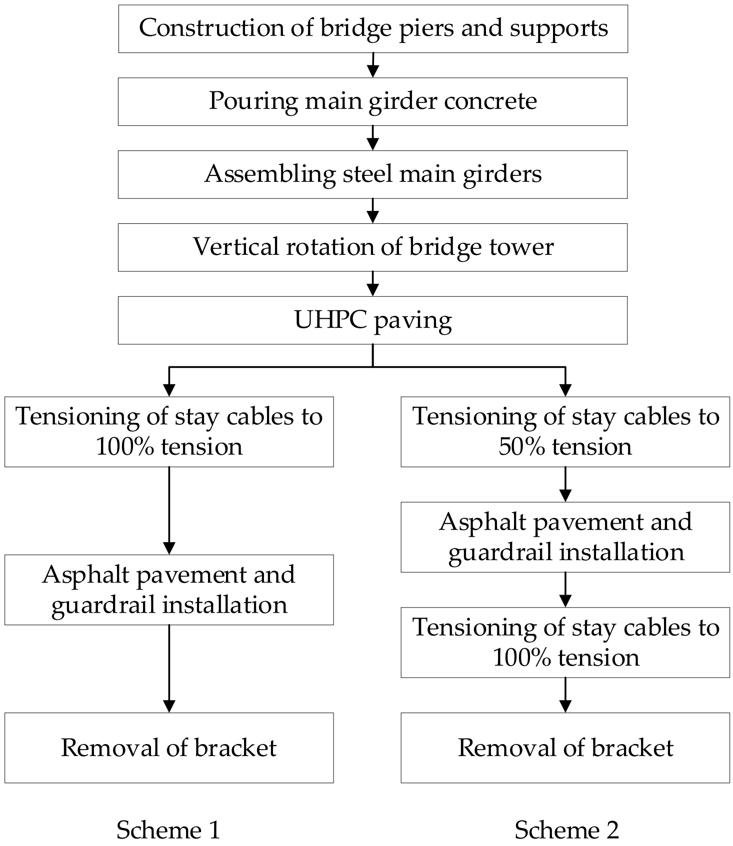

Figure 5 Construction process division

3.3 Comparison of the tensioning cable forces

Based on the design cable force of the bridge, the calculation is performed via the reverse disassembly - positive installation iteration method. First, the reverse disassembly calculation method is used, ignoring the shrinkage and creep of concrete. Then, the positive installation method is performed. The effects of concrete shrinkage and creep are gradually considered according to the construction stage. When the reverse disassembly calculation method is performed again, the shrinkage and creep parameters of concrete determined from the previous positive installation method calculations are used. This process is repeated until the calculation result converges. Table 1 presents a comparison of the two plans.

Table 1 Comparison of the tension cable force and design cable force between the two schemes (Unit: kN)

No.	Design cable force	Cable tension force in scheme I	Cable tension force in scheme II	
			First tension	Second tension
L1	2330	1971	1165	2220
L2	3067	2742	1597	2994
L3	2897	2627	1530	2851
L4	3083	2868	1605	3088
L5	2970	2860	1519	3065
L6	2860	2856	1443	3064
L7	2852	2939	1417	3163
L8	2997	3167	1461	3403
L9	3145	3482	1499	3762

 https://doi.org/10.59238/j.pt.2023.03.006

No.	Design cable force	Cable tension force in scheme I	Cable tension force in scheme II	
			First tension	Second tension
L10	2995	3381	1415	3582
L11	3189	3625	1473	3829
L12	3558	4314	1666	4396
L13	2721	3716	1328	3565
L14	2242	3090	1121	2853
L15	3200	4107	1629	3801
R15	3801	3499	2113	3448
R14	1895	1753	1060	1697
R13	1888	1870	1062	1741
R12	1785	1967	1041	1722
R11	1851	2161	1083	1869
R10	2582	3074	1486	2707
R9	2606	3089	1455	2799
R8	2627	3078	1429	2848
R7	2766	3159	1459	2989
R6	2783	3114	1436	2993
R5	2959	3179	1495	3136
R4	3133	3250	1554	3292
R3	3057	3040	1488	3151
R2	2580	2601	1258	2631
R1	979	1106	490	1030

3.4 Main Girder Stress

3.4.1 Results of scheme I

According to the tensioning scheme of scheme I, the stay cables are sequentially tensioned in the order of L15–L1 and R15–R1. When the stay cables are tensioned to L5, R5, the maximum tensile stress on the bottom concrete girder near the bridge tower is 3.2 MPa. For better clarity, only activate the lower tower column and concrete beam segment elements in Midas. Figure 6 shows the calculation results of the main girder stress.

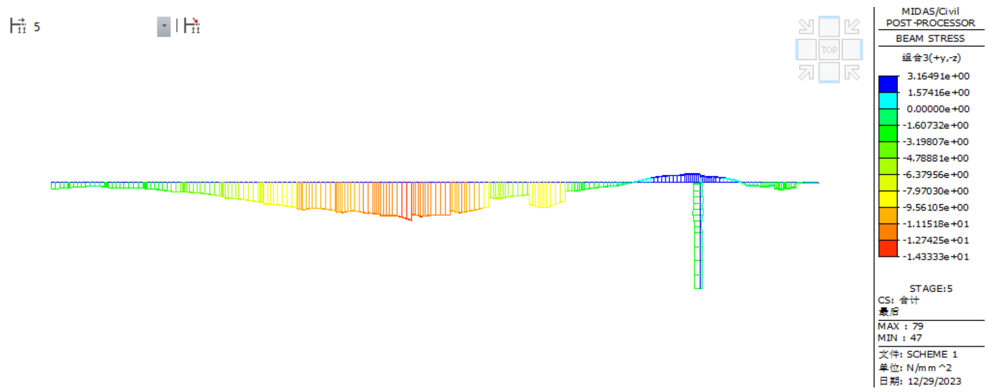

Figure 6 Stresses in the concrete main girder bottom under tension in the L5 and R5 stages (Unit: MPa)

From Figure 7, it can be observed that during the construction process, the maximum compressive stress on the steel main beam is mainly concentrated in the mid-span portion near the abutment, reaching 58.5 MPa. The maximum tensile stress is located on the abutment side of the steel beam, measuring 37.1 MPa. For better clarity, activate only the steel main beam portion in Midas, and the stress calculation results are shown in Figure 7.

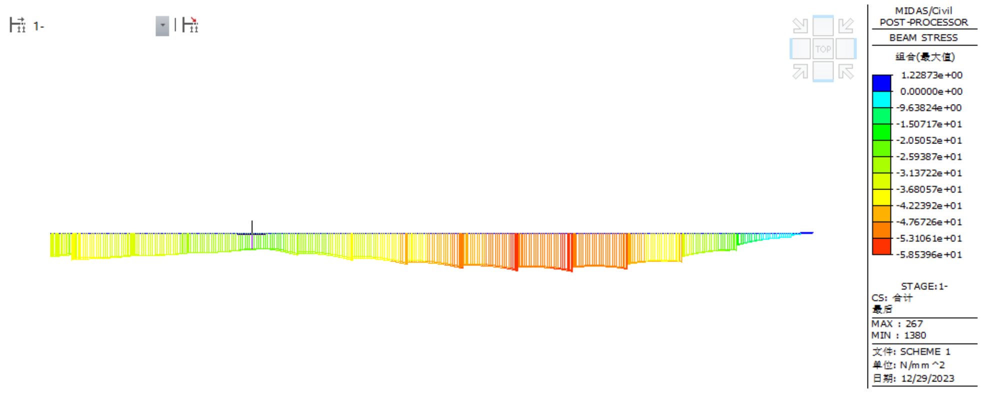

(a) Compressive stress envelope of the steel main girder

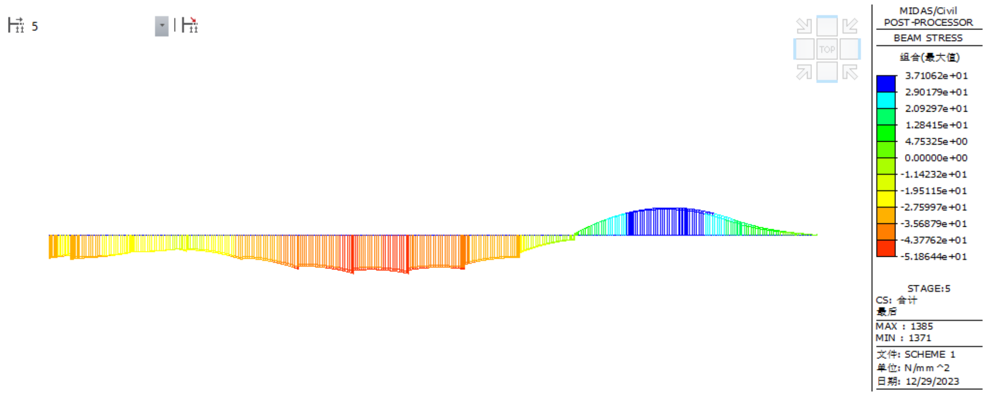

(b) Tensile stress envelope of the steel main girder

Figure 7 Stress envelope diagram of the steel main girder (Unit: MPa)

3.4.2 Results of scheme II

According to the tensioning scheme of Scheme II, the maximum tensile stress on the bottom slab of the concrete main beam occurs during the tensioning at L2, R2. The location is the same as in Scheme I, and the maximum tensile stress is 1.7 MPa. For better clarity, activate only the lower tower columns and the concrete beam segment elements in Midas. The stress calculation results are shown in Figure 8.

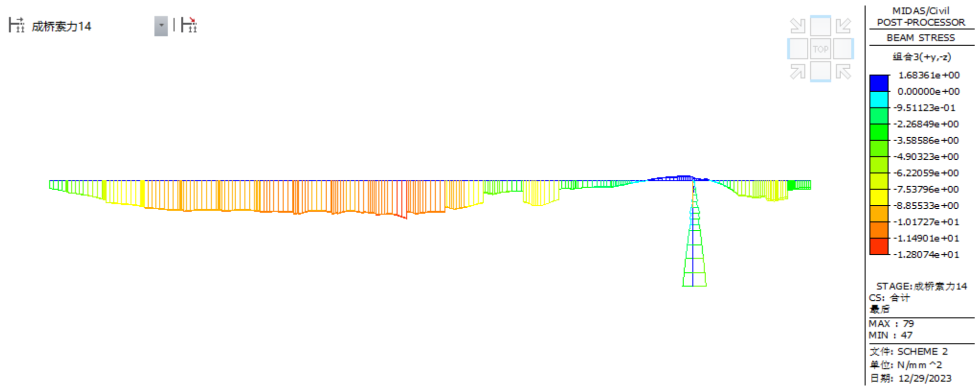

Figure 8 Stresses in the bottom of the concrete main girder in the L2 and R2 stages of tension (Unit: MPa)

As shown in Figure 9, during the construction of the steel main girder, the maximum compressive stress occurs near the bridge pylons at 41.9 MPa. In addition, the

https://doi.org/10.59238/j.pt.2023.03.006

maximum tensile stress occurs at the abutment end of the steel main girder at 13.2 MPa.

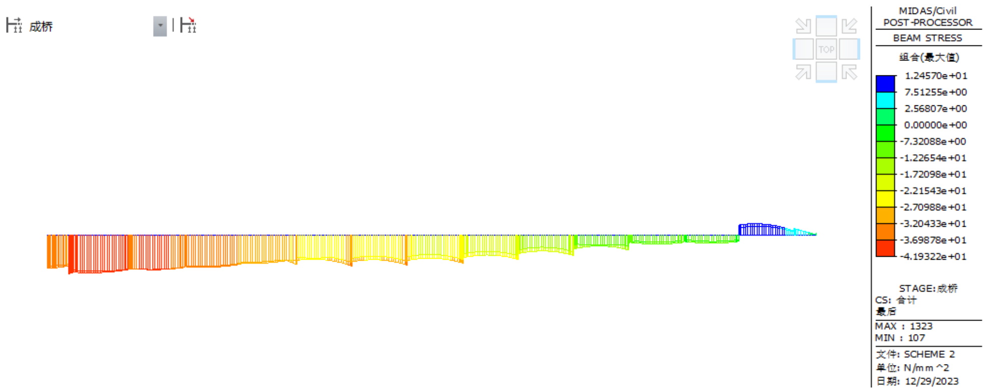

(a) Compressive stress envelope of the steel main girder

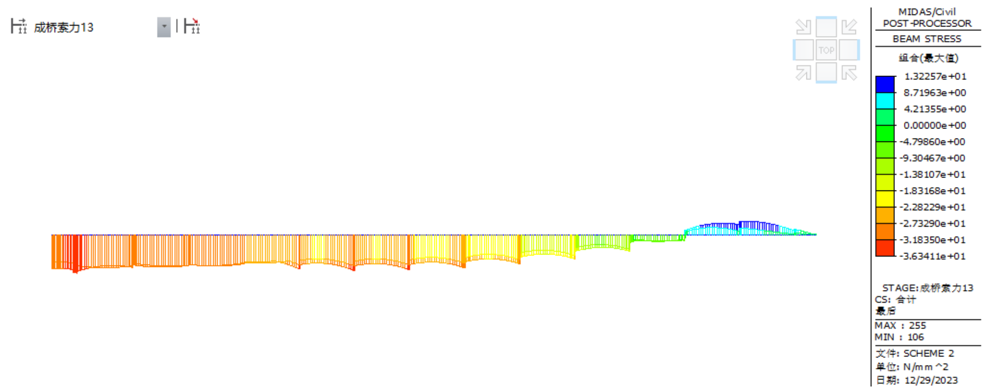

(b) Tensile stress envelope of the steel main girder

Figure 9 Stress envelope diagram of the steel main girder (Unit: MPa)

Through comparison, during the tensioning process, the maximum tensile stress in the concrete main girder bottom of scheme I is 3.2 MPa, which does not meet the monitoring requirements. Moreover, the tensile and compressive stresses of the steel main girder in scheme I are greater than those in scheme II. Therefore, for the bridge, scheme II is safer and more reasonable than scheme I.

4 Comparison of the theoretical calculation values and actual measurement data for scheme II

The Jinwu Bridge adopts the two times cable tensioning scheme recommended in this article for construction tensioning. After the secondary tensioning of the stay cables is completed, the bridge deck asphalt paving, installation of ancillary facilities, and removal of supports, the basic construction of the bridge is completed. The measured values of alignment, stress, and cable forces after the completion of the bridge are compared with the corresponding values in the designed completed bridge state. The results are as follows.

4.1 Bridging stress

The Jinwu Bridge is a hybrid girder cable-stayed bridge, with a total of 8 stress test sections set on its main girder. These sections are named W-1 to W-8, starting from the concrete main girder side at the bridge abutment to the steel main girder side at the bridge abutment, and are located at the following positions: on the girder side 1/4 span, mid-span, and near the abutment-beam junction; on the main span side at the steel-concrete interface (concrete side), 1/4 span of the steel beam, and mid-span of the steel beam. The arrangement of stress monitoring points for each section is illustrated in Figure 10.

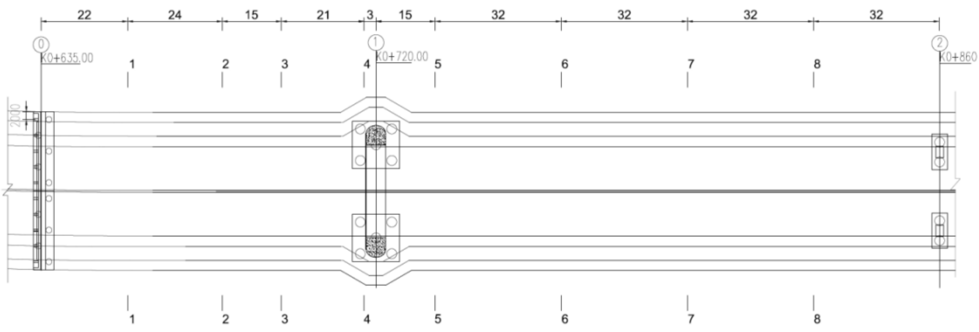

(a) Stress Monitoring Plane Layout Diagram

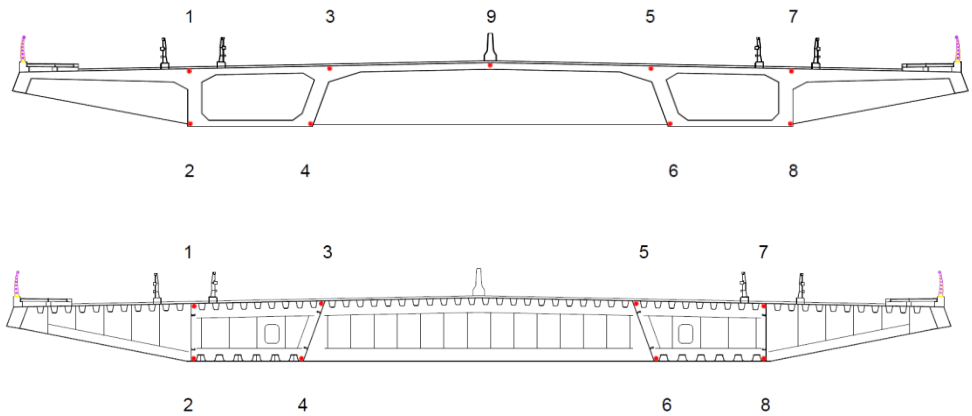

(b) Stress Monitoring Layout Diagram (Transverse Bridge Direction)

Figure 10 Main Girder Stress Measurement Point Layout (Unit: m)

After the completion of the bridge, data measurements were conducted at sensor locations, specifically at the bottom of the deck near the midpoint of each of the 8 selected sections, with measurement point 4. The comparison between the measured data and the theoretical values is shown in Table 2. It can be observed that the stress meets the requirements.

Table 2 Comparison between the theoretical stress and measured stress (Unit: MPa)

Section number	Theoretical stress value	Measured stress value	Error
W-1	-10.2	-9.3	-0.9
W-2	-11.4	-10.3	-1.1
W-3	-14.2	-13.2	-1.0
W-4	-8.3	-7.7	-0.6
W-5	-40.6	-38.5	-2.1
W-6	-30.9	-31.6	1.6
W-7	-25.7	-21.5	-4.2
W-8	-10.9	-12.9	2.0

4.2 Cable force comparison

A comparison of the measured cable forces of the bridge and the target cable forces of the designed bridge is shown in Figure 11, where the deviation is basically within 5%. This deviation meets the requirement. The bridge conditions basically meet the design goal, and no additional cable adjustment needs to be performed on the bridge.

https://doi.org/10.59238/j.pt.2023.03.006

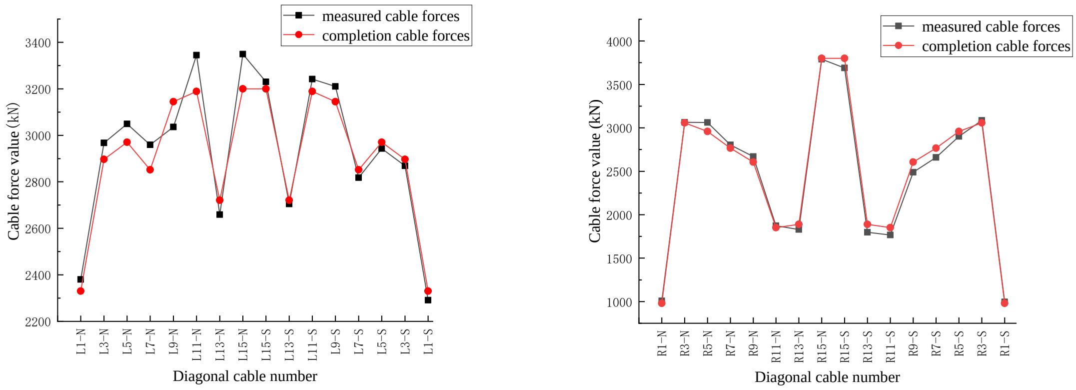

(a) Comparison of the stay cable force of the concrete main girder (b) Comparison of the stay cable force of the steel main girder

Figure 11 Comparison of the cable forces between the actual measurements and design

4.3 Bridge alignment

4.3.1 Main Girder Alignment

To monitor the alignment of the main girder, elevation measuring points are selected at 9 cross-sections of the concrete main girder section and labelled C-1~C-9 in the direction from the side span to the bridge tower. 5 elevation measuring points are selected symmetrically on each cross-section. For the main steel girder section, 14 cross-sections are selected to establish elevation measuring points, and the directions from the side span to the bridge towers are labelled S-1~S-14. Moreover, 5 elevation measuring points are set for each cross-section.

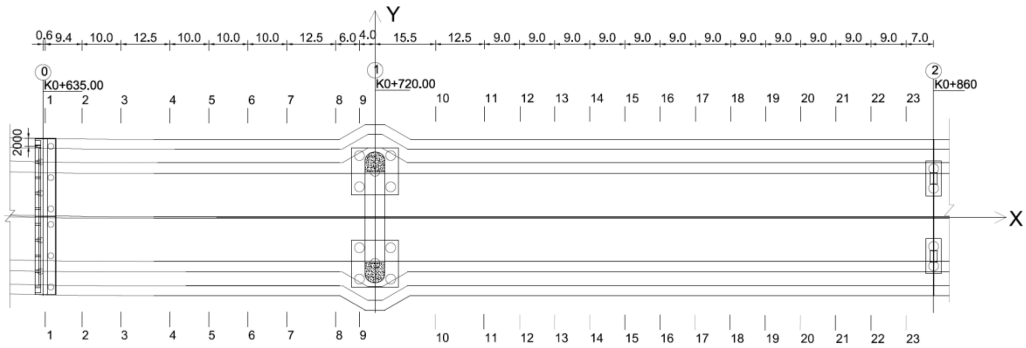

(a) Alignment Monitoring Plane Layout Diagram

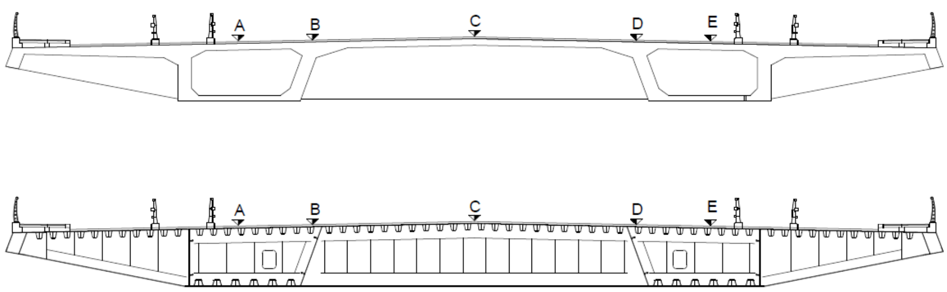

(b) Alignment Monitoring Layout Diagram (Transverse Bridge Direction)

Figure 12 Main Girder alignment Measurement Point Layout (Unit: m)

According to the "specifications for design of highway cable-stayed bridge" (JTG/T 3365-01—2020), the allowable deviation of the top elevation of the main girder of a cable-stayed bridge is $\pm L/5000$, where L is the span. For the bridge, the elevation deviation limit of the concrete main girder is 1.7 cm, and the elevation deviation limit of the steel main girder is 2.8 cm. Based on the data at all measuring points, the maximum deviation between the measured and theoretical values for the concrete main girder is 1.2 cm. The maximum deviation between the measured and theoretical values for the steel main girder is 2.0 cm.

4.3.2 Main Tower Alignment

To monitor the bridge tower alignment, 11 monitoring points were selected at positions 1/8 height, 1/4 height, 3/8 height, 1/2 height, 3/4 height, and tower top on the steel tower. These points are designated as T-1 to T-11 in order from low to high. According to the "specifications for design of highway cable-stayed bridge" (JTG/T 3365-01—2020), the inclination at the top of the pylons of cable-stayed bridges should not exceed 1/3000 of the height of the pylons (2.7 cm). According to the measurement data, the main pylon is deflected to the steel girder side. The maximum vertical deflection of the bridge pylon is 2.3 cm at the T-9 measuring point.

5 Conclusions

Finite element modeling calculations of the Jinwu Bridge were carried out. From the perspective of construction monitoring, two cable tensioning schemes were proposed and compared: the one-time tensioning scheme and the two-time tensioning scheme. The following conclusions were drawn:

(1) In the one-time tensioning scheme, the maximum tensile stress in the concrete main girder bottom was 3.2 MPa, and the stress in the steel main girder ranged from -58.7 MPa to 37.1 MPa. In the two-time tensioning scheme, the calculation result of the concrete main girder bottom was 1.7 MPa. The stress range of the steel main girder was -41.9 MPa~13.2 MPa. Therefore, the two-time tensioning scheme was conducive to bridge stress control during construction.

(2) The two-time tensioning scheme was adopted for the Jinwu Bridge. The maximum deviation between the measured and theoretical values for the alignment of the concrete main girder was 1.2 cm, and the maximum deviation for the alignment of the steel main girder was 2.0 cm. The main tower was deflected to the steel girder side, and the maximum vertical displacement of bridge of the measuring point compared to the pre-tensioning level was 2.3 cm. These values met the monitoring requirement. The measured stresses of the full bridge deviated from the theoretical values and were both within the safe range. The deviation between the actual measured cable force and the target cable force of the designed bridge had to be within 5%. The bridge condition reached the design goal, and there was no need for cable adjustment.

(3) For this bridge, a two-times tensioning scheme (Scheme II) is employed, where the first tensioning is carried out up to 50% of the design cable force. After the completion of the second-phase pavement, the second tensioning is performed, extending to 100% of the cable force. Compared to a one-time tensioning scheme reaching 100% of the cable force (Scheme I), this two-times tensioning scheme is more advantageous for safety and alignment control during bridge construction. A more in-depth analysis of the proportional relationship between the first and second-stage tensioning forces in scheme II can be conducted to derive the optimal tensioning strategy.

Conflict of Interest: All authors disclosed no relevant relationships.

Data Availability Statement: The data that support the findings of this study are available from the corresponding author, Li, upon reasonable request.

References

1. Zhan, J.; Zhang, M. *Prestressed Concrete Partial Cable-stayed Bridge*; China Communications Press Co., Ltd.: 2016.
2. Wang, J.; Xu, J.; Dai, Z. Construction Techniques for Stay Cables of Xichang Cable-Stayed Bridge in Tonghua. *Bridge Construction* **2006**, 77-80, doi:10.3969/j.issn.1003-4722.2006.z1.025.
3. Zhou, H.; Xiong, S. Optimization Scheme of Stay Cable Adjustment for Main Bridge of Nancang Avenue Interchange in Tianjin. *Bridge Construction* **2010**, 36-39.
4. Liang, P.; Xiao, R.; Xu, Y. Random Simulation Analysis of Construction Process for Super-Long-Span Cable-Stayed Bridges. *China Journal of Highway and Transport* **2006**, 52-58, doi:10.19721/j.cnki.1001-7372.2006.04.010.
5. Zheng, Z.; Xiang, Y.; Zhu, W. Determination and Optimization of Cable Stresses during Construction for Cable-stayed Bridge. *China Municipal Engineering* **2002**, 28-31, doi:10.3969/j.issn.1004-4655.2002.03.009.
6. Duan, R.; Ran, Z.; Wang, X.; Bai, Y. Study of the Backfill Effect on Tunnel Lining Segments Property. *Journal of Xi'an University of Architecture & Technology(Natural Science Edition)* **2019**, *51*, 59-66+82, doi:10.15986/j.1006-7930.2019.01.010.
7. Wei, D.; Peng, X.; Tao, L.; Yin, G. Optimization and Analysis of Tensioned Stay Cable Forces in Construction of Liuguang River Bridge. *Bridge Construction* **2017**, *47*, 36-41, doi:10.3969/j.issn.1003-4722.2017.06.007.

AUTHOR BIOGRAPHIES

	**Quan Zhang** M.E. student, Department of Bridge Engineering, School of Civil Engineering, Tongji University. Research Direction:Bridge Engineering. Email: 820100664@qq.com		**Xianjing Li** M.E.,Chief Engineer of the Bridge Branch of the Municipal Transportation Design and Research Institute of Lin Tung-Yen & Li Guo-Hao Consultants Shanghai Co., Ltd. Research Direction: Bridge Engineering Design and Consulting. Email: 87345436@qq.com
	**Jishu Wu** Ph.D. student, Department of Bridge Engineering, School of Civil Engineering, Tongji University. Research Direction:Bridge Engineering. Email: wujishucn@gmail.com		**Chao Liu** Ph.D., Associate Professor, Department of Bridge Engineering, School of Civil Engineering, Tongji University. Graduated from Tongji University in 2006. Research Direction: Intelligent Monitoring, Bridge Fine Design Theory. Email: lctj@tongji.edu.cn